

## Article

# Paraoxonase-1 and -3 protein expression in brain of the Tg2576 mouse model of Alzheimer's disease

Jose Gregorio Salazar <sup>1,2,3†</sup>, Judit Marsillach <sup>4,5†</sup>, Ingrid Reverte <sup>1,2,6,7</sup>, Bharti Mackness <sup>8</sup>, Michael Mackness <sup>8</sup>, Jorge Joven <sup>4</sup>, Jordi Camps <sup>4,\*</sup> and Maria Teresa Colomina <sup>1,2,\*</sup>

<sup>1</sup> Department of Psychology and Research Center for Behavioral Assessment (CRAMC), Universitat Rovira i Virgili, Tarragona 43007, Spain; [mariateresa.colomina@urv.cat](mailto:mariateresa.colomina@urv.cat) (M.T.C.)

<sup>2</sup> Research in Neurobehavior and Health (NEUROLAB), Universitat Rovira i Virgili, Reus 43201, Spain; [mariateresa.colomina@urv.cat](mailto:mariateresa.colomina@urv.cat) (M.T.C.)

<sup>3</sup> Current address (J.G.S.): Departamento de Toxicología y Farmacología, Facultad de Farmacia y Bioanálisis, Universidad de Los Andes, Mérida 5101, Venezuela; [salazarjg@ula.ve](mailto:salazarjg@ula.ve)

<sup>4</sup> Unitat de Recerca Biomèdica, Hospital Universitari de Sant Joan, Institut d'Investigació Sanitària Pere Virgili, Universitat Rovira i Virgili, Reus 43201, Spain; [jjoven@grupsagessa.com](mailto:jjoven@grupsagessa.com) (J.J.); [jcamp@grupsagessa.com](mailto:jcamp@grupsagessa.com) (J.C.)

<sup>5</sup> Current address (J.M.): Department of Environmental and Occupational Health Sciences, University of Washington, Seattle WA, 98195, United States; [jmars@uw.edu](mailto:jmars@uw.edu)

<sup>6</sup> Current address (I.R.): Department of Physiology and Pharmacology, Sapienza University of Rome, Rome 00185, Italy; [ingrid.reverte@uniroma1.it](mailto:ingrid.reverte@uniroma1.it)

<sup>7</sup> Current address (I.R.): Santa Lucia Foundation (IRCCS Fondazione Santa Lucia), Rome 00179, Italy; [ingrid.reverte@uniroma1.it](mailto:ingrid.reverte@uniroma1.it)

<sup>8</sup> Miami Platja, Tarragona, Spain; [mike.mackness@gmail.com](mailto:mike.mackness@gmail.com) (B.M. and M.M.)

\* Correspondence: [jcamp@grupsagessa.com](mailto:jcamp@grupsagessa.com) (J.C.); [mariateresa.colomina@urv.cat](mailto:mariateresa.colomina@urv.cat) (M.T.C.); Tel.: +34-977-558153 (M.T.C.)

† These authors contributed equally to this work.

**Abstract:** Background: Brain oxidative lipid damage and inflammation are common in neurodegenerative diseases such as Alzheimer's disease (AD). Paraoxonase-1 and 3 (PON1 and PON3) protein expression have been described in tissues with no *PON1* and *PON3* gene expression. In the present study, we aimed to examine differences in PON1 and PON3 protein expression in the brain of a mouse model of AD. Methods: We used peroxidase-based and fluorescence-based immunohistochemistry in 5 brain regions (olfactory bulb, forebrain, posterior midbrain, hindbrain and cerebellum) of transgenic (Tg2576) mice with the Swedish mutation (KM670/671NL) responsible for a familial form of AD and corresponding wild-type mice. Results: We found intense PON1 and PON3 positive staining in star-shaped cells surrounding A $\beta$  plaques in all Tg2576 mouse brain regions studied. Although we could not co-localize PON1 and PON3 with astrocytes, brain star-shaped cells, we found some co-localization of PON3 with microglia. Conclusions: These results suggest that 1) PON1 and PON3 cross the blood-brain barrier in discoidal HDLs and are transferred to specific brain cell types, and 2) PON1 and PON3 play an important role in preventing oxidative stress and lipid peroxidation in particular cell types, likely astrocytes and microglia, in AD pathology, and potentially in other neurodegenerative diseases.

**Keywords:** paraoxonases; oxidative stress; Alzheimer's disease; brain; Tg2576 mice; astrocytes; hippocampus; amyloid- $\beta$ ; microglia; neurons

## 1. Introduction

Alzheimer's disease (AD) is the most frequent form of dementia in the elderly contributing to 60–70% of all dementia cases [1]. It is characterized by a progressive mental deterioration of functions at several cognitive domains, while neuropathological signs build up gradually in several cortical

regions of the brain [2]. There are two forms of AD: the familial form, which is less frequent (1–5%), and the late-onset AD form, which is most prevalent and appears later in life [3]. The former encompasses different genetic variants affecting the processing of the amyloid beta precursor peptide (APP). Different mutations at the APP or at the cleaving enzymes presenilin 1 or presenilin 2 have been described to contribute to the amyloid cascade hypothesis for AD [3]. One of the most prominent and first appearing neuropathological signs of AD is the presence of amyloid- $\beta$  (A $\beta$ ) plaques. These senile plaques consist in a central core of amyloid  $\beta$  insoluble 39–42 residue peptides fragments, surrounded by astrocytes, microglia and nearby neurons. A $\beta$  in its oligomeric form is toxic and is known to induce oxidative stress, while A $\beta$  aggregates complexed with the redox metal ion copper (Cu) maintain its ability to increase hydroxyl radicals formation [4]. Moreover, A $\beta$  aggregates interact with cell membranes, favor the entrance of Ca, and have been implied in synaptic loss, and apoptosis [4]. Further, AD patients frequently suffer vascular complications including cerebrovascular amyloid angiopathy and atherosclerosis [5]. There are currently several AD mouse models based in human genetic early-onset forms of AD. The Swedish Tg2576 transgenic mouse is one of the most used AD mouse models. This mouse overexpresses a mutant form of human APP (isoform 695) in addition to containing the Swedish mutation (KM670/671NL), leading to an increase of A $\beta$  1-40 and 1-42 fragments and the formation of A $\beta$  plaques in brain [6]. In addition to a high-level expression of the mutant A $\beta$  peptide, the Tg2576 mice show a behavioral phenotype characterized by spatial memory deficits at 9 months of life and beyond and increased microglial density and number of A $\beta$  plaques in frontal, temporal and entorhinal cortex, and hippocampus. Aged Tg2576 mice also show brain oxidative lipid damage surrounding A $\beta$  deposits [7].

The paraoxonase (PON) family of enzymes comprises 3 members, paraoxonase-1 (PON1), PON2 and PON3. In humans, *PON1* and *PON3* are expressed in the liver and at lower levels in the kidney, and their protein products are mainly found in circulating high-density lipoproteins (HDLs) [8–10] and in endoplasmic reticulum of intestinal cells [11]. PON3 protein expression has also been described in mitochondria of selected tissues [12]. It has been hypothesized that HDLs could act as delivery carrier of PON1 (and likely PON3) from liver to tissues where its activity is needed, based on reports of PON1 transfer to membranes [13–15] and the presence of PON1 and PON3 in certain tissues with no demonstrated *PON1* and *PON3* gene expression [16–19]. All PONs are polymorphic enzymes, with certain polymorphisms affecting their activity or protein expression (reviewed in [20,21]). The physiological roles of these enzymes are still uncertain, although it is accepted that they are lactonases with broad substrate specificity [22,23]. The three PONs are potent antioxidant, anti-inflammatory and anti-apoptotic enzymes. PON1 and PON3 also participate in the HDL-mediated cholesterol efflux from macrophages, in a mechanism that involves the ATP-binding cassette A-1 (ABCA-1) receptor, contributing to an important atheroprotective role [24–27]. Alterations in circulating plasma PON1 levels have been reported in a variety of oxidative stress-related diseases. These include cardiovascular disease, chronic renal failure, HIV-infection, metabolic syndrome, chronic liver impairment, and AD, among others [21,28,29].

Substantial evidence indicates that oxidative stress is involved in the pathogenesis and progression of AD [30–32]. In monomeric form, A $\beta$  peptides have antioxidant activity; however, when A $\beta$  peptides form aggregates, they exhibit pro-oxidant activity, thus promoting oxidative stress [33]. In AD, lipid peroxidation seems to be a major contributor to oxidative stress damage due to the brain's high oxygen consumption and high content of polyunsaturated fatty acids [34]. Presence of oxidative stress products has been described in brain regions with AD histopathologic alterations [35]. Interestingly, brain antioxidant enzyme activities significantly increase in areas of lipid peroxidation, suggesting a compensatory response to increased oxidative stress [36]. Although there is no *PON1* or *PON3* gene expression in brain, we identified PON1 and PON3 protein expression in white matter brain areas of healthy C57BL/6J mice [18]. Thus, PON1 and PON3 could play an important role in modulating brain oxidative stress during AD progression.

The aim of the present study was to examine differences in the presence of PON1 and PON3 protein in brains of aged Tg2576 mice with presence of A $\beta$  plaques compared with brains of WT mice with no A $\beta$  plaques. Our hypothesis was that during AD progression, protein expression of PON1

and PON3 would increase in brain regions with high oxidative stress, that have been described to coincide with increased presence of A $\beta$  plaques. We found very intense expression of PON1 and PON3 exclusively surrounding A $\beta$  plaques and in star-shaped cells located around those areas.

## 2. Materials and Methods

### 2.1 Animals

Male transgenic (Tg2576) mice with the Swedish mutation (KM670/671NL) responsible for a familial form of AD were obtained from Taconic Europe [Lille Skensved, Denmark; strain name: B6;SJL-Tg(APP<sup>SWE</sup>)2576Kha]. Corresponding wild-type (WT) mice were generated by crossing parental APP<sup>Swe</sup> heterozygous male mice (Taconic Europe) with C57BL6/SJL female mice (Charles River, Barcelona, Spain). For the proposed experiments, mice were genotyped by PCR using DNA extracted from mouse tail at 2 months of age and separated according to their gender and genotype. Mice were maintained in an animal room with standard conditions: a light/dark cycle of 12:12 h, a temperature of 22 $\pm$ 2 °C and a relative humidity of 50  $\pm$  10%. All mice had food (standard chow diet, Panlab, Barcelona) and drinking water available *ad libitum*. The experimental protocol was approved by the Animal Care and Use Committee of the *Universitat Rovira i Virgili*, Tarragona, Spain (ethical approval code number 239, URV2014).

At eighteen months old, 2 Tg2576 and 2 WT mice were sacrificed. After being anesthetized (xylazine 10 mg/kg and ketamine 100 mg/kg, i.p.), mice received intracardiac perfusion perfused with 0.9% NaCl followed by 4% paraformaldehyde (PFH). Brains were carefully removed and placed in 4% PFH at 4 °C for 2 h, then sectioned in coronal sections by an adult mouse brain slicer matrix BSMAS001-1 (Zivic instruments, US) and the following regions separated: olfactory bulb, forebrain, posterior midbrain, hindbrain and cerebellum. These brain regions were then dehydrated and embedded in paraffin, and 2 cm-thickness coronal brain sections were obtained for all histological analyses.

### 2.2. Antibodies

The polyclonal rabbit anti-mouse PON1 and PON3 antibodies were obtained as previously described [18], using peptides derived from specific sequences of mature PON1 or PON3. These antibodies are specific for each PON protein. The other antibodies used were obtained commercially as detailed below.

### 2.3. Peroxidase-based immunostaining

Brain sections from each region were deparaffinized and rehydrated using standard protocols. The buffer used throughout the protocol was 20 mM Gly, 100 mM PBS pH 7.4. Rehydrated sections were rinsed in 0.1% Triton X-100 (Sigma-Aldrich, Barcelona, Spain) in Gly-PBS buffer, and incubated in H<sub>2</sub>O<sub>2</sub> for 10 min to inactivate endogenous peroxidases. Then, sections were blocked for 30 min in 2% bovine serum albumin (BSA, Sigma-Aldrich) in 0.1% Triton X-100, Gly-PBS buffer. Blocking buffer was carefully removed by tapping the slide on filter paper, prior to addition of the primary antibodies. Anti-PON1 or anti-PON3 antibodies diluted 1:300 v/v in 1% BSA, 0.1% Triton X-100, Gly-PBS buffer were applied over tissue sections and incubated in a humid chamber o/n at 4 °C. After a 10 min wash with 0.1% Triton X-100, Gly-PBS buffer, sections were incubated for 1 h with a biotinylated anti-rabbit antibody (Vector Laboratories, Barcelona, Spain) diluted 1:200 v/v in 1% BSA, 0.1% Triton X-100, Gly-PBS buffer. We used the immunoenzymatic antigen detection system Vectastain ABC kit, followed by the DAB Peroxidase (HRP) Substrate kit (both from Vector Laboratories), yielding an insoluble brown-colored product in areas with antigen-antibody recognition. We used these two kits as suggested by the manufacturer. Sections were counterstained with haematoxylin for 30 s, dehydrated using standard procedures and preserved using DPX resin as mounting media (Sigma-Aldrich). Slides were visualized using an upright widefield microscope (Eclipse 600, Nikon, Barcelona, Spain). Pictures were obtained using the AnalySIS image software system (Soft Imaging System, Munster, Germany). Negative control slides were stained following the same protocol but omitting incubation with primary antibodies.

### 2.3. Fluorescence-based immunostaining

After removing paraffin and rehydrating sections using standard protocols, brain slides were rinsed in 0.1% Triton X-100, Gly-PBS buffer (same Gly-PBS buffer detailed above). Slides were then blocked for 30 min in blocking buffer (2% BSA in 0.1% Triton X-100, Gly-PBS buffer). After removing blocking buffer by tapping on a filter paper, slides were incubated overnight at 4 °C in a humid chamber with either of the following primary antibodies: 1/300 rabbit polyclonal anti-PON1, 1/300 rabbit monoclonal anti-PON3, 1/160 mouse monoclonal anti-glial fibrillary acidic protein, GFAP (Calbiochem, Darmstadt, Germany), 1/200 mouse monoclonal anti-neuronal nuclei, NeuN (Millipore, Temecula, USA), 1/100 rat monoclonal anti-neuroectodermal stem cell marker, Nestin (Millipore), 1/300 goat polyclonal anti-ionized calcium-binding adapter molecule 1, Iba1 (Santa Cruz Biotechnology, Santa Cruz, USA) and 1/500 mouse monoclonal anti-beta amyloid (Sigma-Aldrich). After 2x10 min wash with 0.1% Triton X-100, Gly-PBS buffer, slides were incubated for 3 h at room temperature in a humid chamber with either of the following secondary antibodies: 1/500 anti-rabbit fluorescein isothiocyanate (FITC)-conjugated (AlexaFluor 488, Invitrogen, Carlsbad, USA), 1/400 anti-mouse tetramethyl rhodamine isothiocyanate (TRITC)-conjugated (AlexaFluor 568, Invitrogen, Carlsbad, USA) and 1/400 anti-goat Cy5-conjugated (Santa Cruz Biotechnology). Both primary and secondary antibodies were diluted in 1% BSA, Gly-PBS buffer. Final wash was applied, and sections were mounted with the addition of an antifading reagent (*SlowFade* Gold Antifade Reagent, Invitrogen, Carlsbad, USA), and stored until observation in a laser-scanning confocal microscopy (Nikon NIS-Elements Eclipse TE2000E, Nikon Corp, Tokyo, Japan). Images were adjusted for brightness and contrast using Adobe Photoshop (Adobe Systems, San Jose, USA). Negative control slides were stained following the same protocol but omitting incubation with primary antibodies. Additionally, a secondary antibody negative control was also prepared by omitting the secondary antibody in the incubation instead of the primary antibody.

### 3. Results

#### 3.1. PON1 and PON3 peroxidase-based immunohistochemistry

PON1 and PON3 peroxidase-based immunohistochemistry resulted in a moderate staining (brown) localized in brain white matter fiber tracts, especially in corpus callosum and in internal and external capsule, in both WT and Tg2576 mice. The presence of PON1 and PON3 in WT mice was scarce and mainly located near myelinated tracts, as already described [18]. In the brain of Tg2576

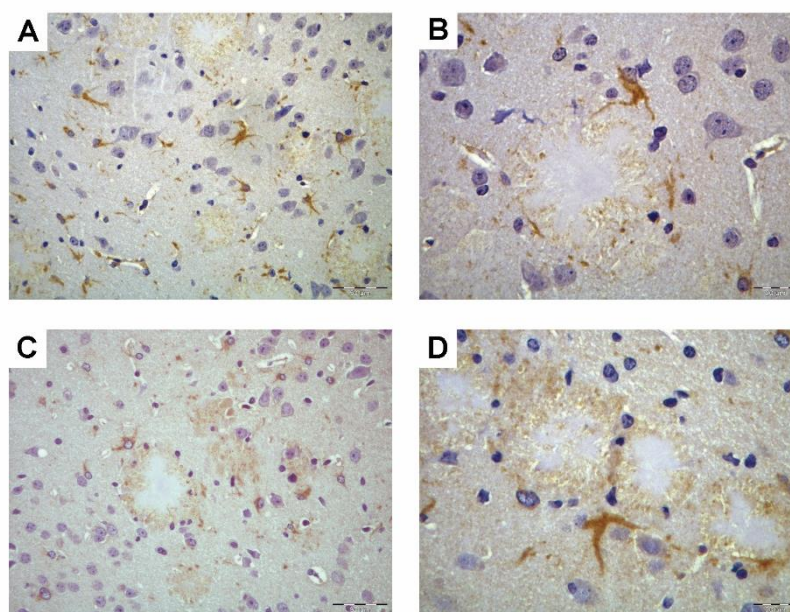


**Figure 1.** PON1 and PON3 peroxidase-based immunohistochemistry in the parietal cortex of the posterior midbrain region of aged Tg2576 mice. **A:** PON1 immunohistochemistry, 200x magnification. **B:** PON1 immunohistochemistry, 400x magnification. **C:** PON3 immunohistochemistry, 200x magnification. **D:** PON3 immunohistochemistry, 400x magnification.



mice, in addition to myelinated tracts, both PON1 and PON3 staining were highly concentrated around A $\beta$  plaques located mainly in the hippocampus, and parietal and temporal cortex (**Figure 1**). These images showed also the presence of intense PON1 and PON3 immunostaining in some cells morphologically compatible with astrocytes or microglial cells, surrounding A $\beta$  plaques. The negative control slides showed no positive (brown) staining (data not shown).

### 3.2. Fluorescence-based immunohistochemistry

#### 3.2.1. PON1 and PON3 immunofluorescence

We used PON1 and PON3 fluorescence-based immunohistochemistry, or immunofluorescence, to ensure we could reproduce the results obtained using peroxidase-based immunohistochemistry. As depicted in **Figure 2**, PON1 and PON3 immunofluorescence showed some background staining in the form of small very bright green precipitates that could be seen in all slides analyzed (negative antibody controls, WT and Tg2576 mice). For the primary and secondary antibody negative control slides, we used Tg2576 mouse brain sections (**Figure 2A-B**, respectively). WT mouse brain showed positive staining (green) in myelinated tracts in both PON1 and PON3 immunofluorescence (**Figure 2C-D**, respectively), as already reported using peroxidase-based immunohistochemistry [18]. In Tg2576 mice, PON1 and PON3 positive staining (green) was found surrounding A $\beta$  plaques and in cells with a star shape in all brain sections with presence of A $\beta$  plaques analyzed (**Figure 2E-F**, respectively). All the sections depicted in **Figure 2** were obtained from parietal cortex areas of the posterior midbrain region.

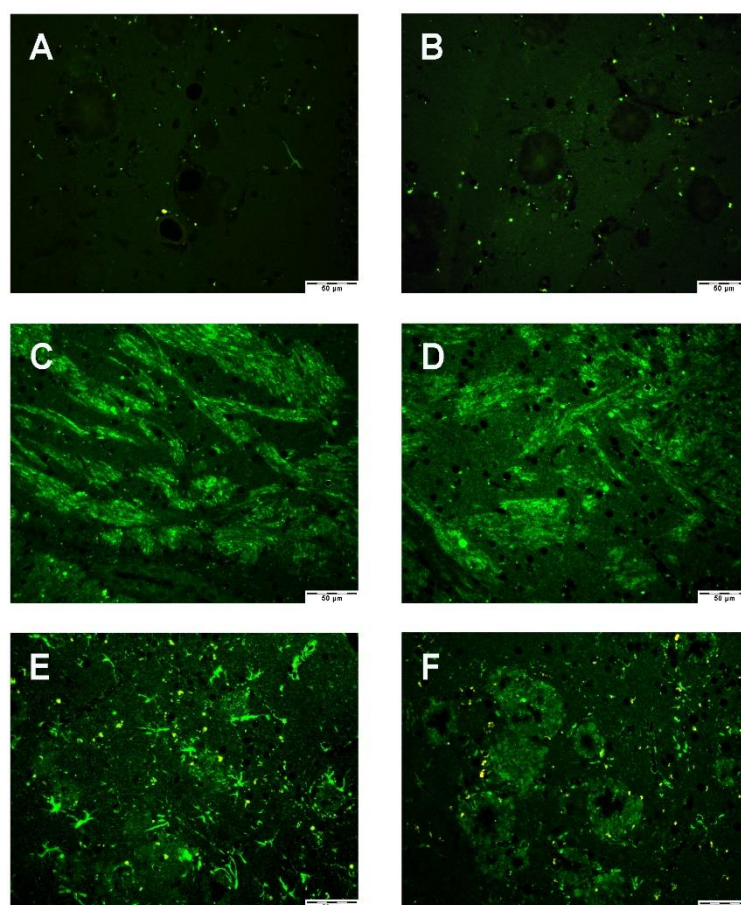


**Figure 2.** PON1 and PON3 immunofluorescence in the parietal cortex of the posterior midbrain region. All panels are at 200x magnification. **A:** PON1 immunofluorescence, omitting the primary antibody in Tg2576 mice. **B:** PON1 immunofluorescence omitting the secondary antibody in Tg2576 mice. **C:** PON1 immunofluorescence in WT mice. **D:** PON3 immunofluorescence in WT mice. **E:** PON1 immunofluorescence in Tg2576 mice. **F:** PON3 immunofluorescence in Tg2576 mice.

### 3.2.2. Astrocyte-microglia-neuron “triad” immunofluorescence

Triple immunofluorescence was conducted to ensure proper labeling of A $\beta$  plaques and their surrounding cells (astrocytes, microglia and proliferating neurons). As seen in **Figure 3A**, A $\beta$  deposition (in blue) was surrounded by a large number of star-shaped cells, corresponding to astrocytes (GFAP, green) and several microglia (Iba1, red). **Figure 3B** shows A $\beta$  deposition (in red) was surrounded by astrocytes (GFAP, green) and some proliferating neurons (Nestin, purple). The GFAP positive staining in **Figure 3** resembled the PON1 and PON3 positive staining in **Figure 2E** and **2F**.

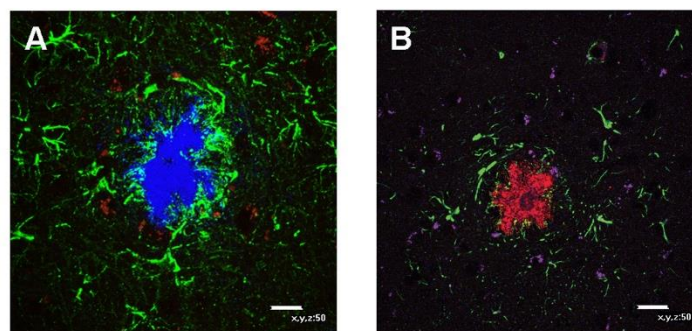


**Figure 3.** Triple immunofluorescence in the parietal cortex of the posterior midbrain section of Tg2576 mice. A: astrocyte (GFAP, green) – microglia (Iba1, red) – A $\beta$  deposition (blue) immunofluorescence, obtained using different lasers and merged. B: astrocyte (GFAP, green) – neuron (Nestin, purple) – A $\beta$  deposition (red) immunofluorescence, obtained using different lasers and merged. All panels are at 400x magnification.

### 3.2.3. PON1 and astrocyte-microglia-neuron “triad” double immunofluorescence

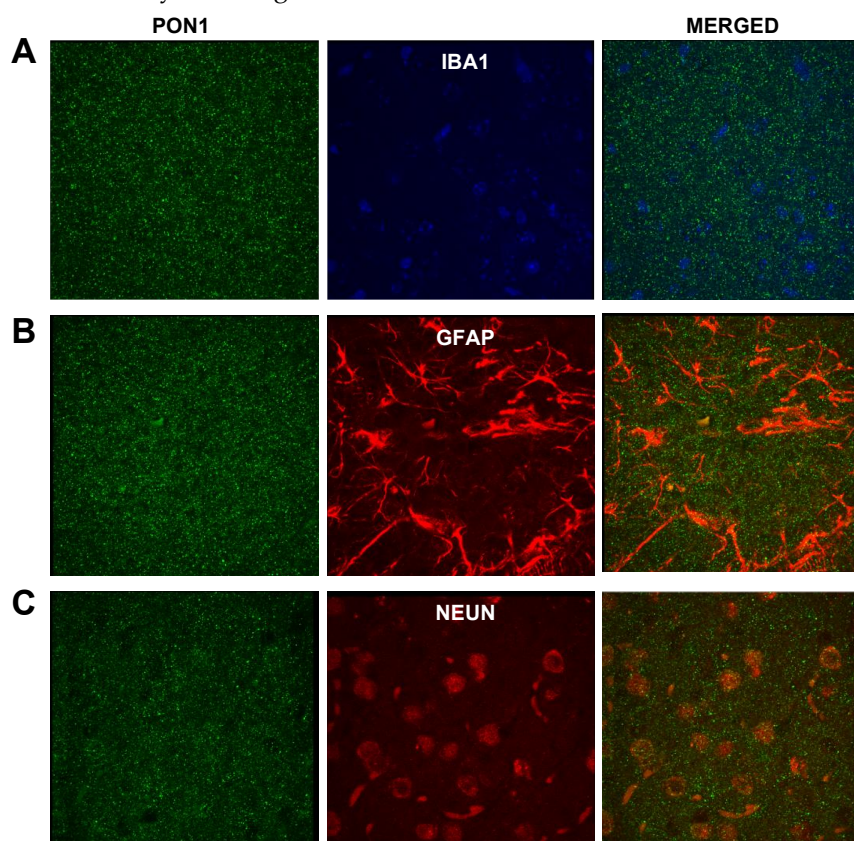


**Figure 4.** Double immunofluorescence of PON1 and brain cell markers for **A:** microglia (Iba1); **B:** astrocytes (GFAP); and **C:** neurons (NeuN) in sections from Tg2576 mouse brain temporal cortex; 1000x magnification.



We carried out double immunofluorescences targeting PON1 and individual brain cell markers, to determine if there is co-localization of PON1 with any of the cell types found surrounding A $\beta$  plaques. We focused on the astrocyte-microglia-neuron “triad” and used the following specific cell markers: GFAP for astrocytes, Iba1 for activated microglia, and NeuN for neuronal nuclei. Surprisingly, we did not see co-localization between PON1 and any of the 3 cell markers used in each double immunofluorescence (PON1 and Iba1, PON1 and GFAP, or PON1 and NeuN) (**Figure 4**). It should be noted that PON1 immunofluorescence showed a significant amount of non-specific background staining, in comparison with the results obtained in single PON1 immunofluorescence (**Figure 2A, C and E**), that made it difficult to differentiate it from any specific staining.

#### 3.2.4. PON3 and astrocyte-microglia-neuron “triad” double immunofluorescence

When targeting PON3 and individual components of the astrocyte-microglia-neuron “triad”, we only found some co-localization with microglia (**Figure 5A**). PON3 co-localized with certain areas of the microglia’s cytoplasm. We did not see co-localization with markers of astrocytes or neurons (**Figure 5B and 5C**). As seen with PON1, PON3 double immunofluorescence also showed a significant degree of non-specific staining.

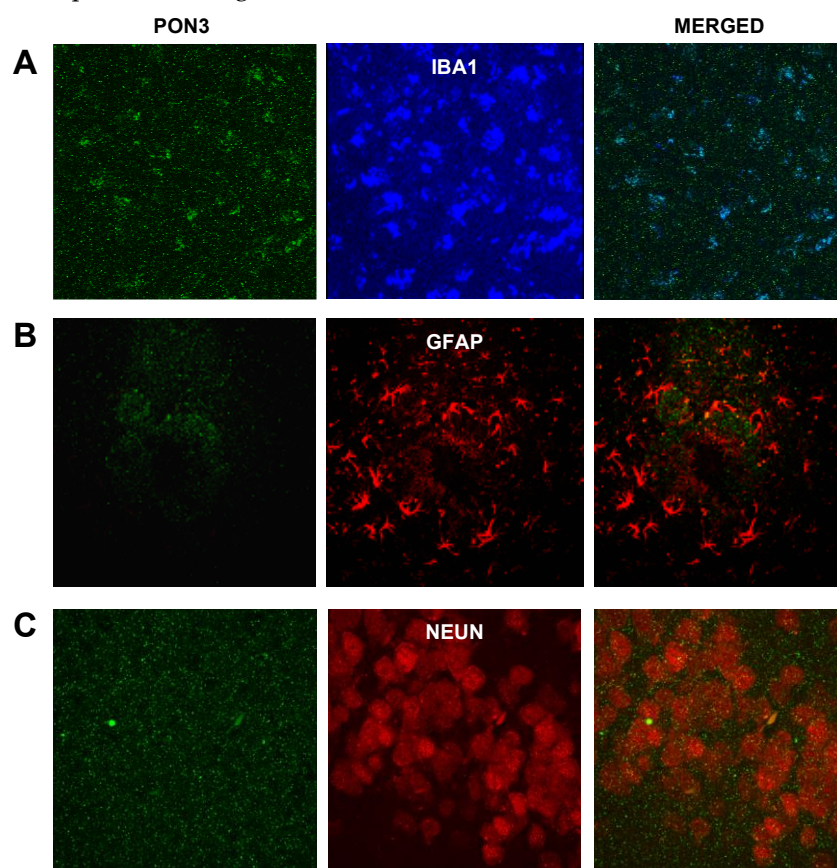


**Figure 5.** Double immunofluorescence of PON3 and brain cell markers for **A:** microglia (Iba1); **B:** astrocytes (GFAP); and **C:** neurons (NeuN) in sections from Tg2576 mouse brain temporal cortex; 1000x magnification.

## 4. Discussion

In the present study, the possibility of a differential expression of PON1 and PON3 in brain of healthy mice and mice with AD pathology was evaluated. Although our results are not conclusive, we show strong evidence of PON1 and PON3 expression surrounding A $\beta$  plaques, as well as intense positive staining in star-shaped cells that resemble astrocytes, in areas with abundance of A $\beta$  plaques.

This is the first report describing PON1 and PON3 protein localization in these cells and regions in mouse AD pathology, compared with healthy mice.

Although there is no documented *PON1* or *PON3* gene expression in any of the mouse or human brain regions, earlier evidence already reported PON1 and PON3 protein is expressed in myelinated fibers in brain tissue of healthy C57BL/6 mice [18], suggesting that PON1 and PON3 are somehow transferred from blood circulation to the brain. In the same year, another group demonstrated, for the first time, presence of PON1 activity in human cerebrospinal fluid [37], with more recent articles reporting decreased cerebrospinal fluid PON1 activity in dementia and AD patients [38,39]. Altogether, this would strongly support transfer of PON1, and PON3, from blood circulation to the central nervous system. Indeed, *in vitro* studies have shown that small HDL particles are transcytosed across the blood-brain barrier via scavenger receptor class B, type I (SR-B1)-mediated uptake [40,41]. We hypothesize that PON1 and PON3, embedded in discoidal HDLs, would cross the blood-brain barrier and be transferred to these AD pathological brain areas and cells via an unknown mechanism [15].

Astrocytes are star-shaped glial cells that have an important role in the synthesis of cholesterol, lipoprotein components and assembly of lipoproteins in the brain. Astrocytes also participate in the cholesterol efflux to lipoproteins, regulated by ATP-binding cassette transporters A-I (ABCA-1) and G-I (ABCG1). As plasma HDL-bound PON1 and PON3 participate in the cholesterol efflux from macrophages to HDL, the suggested presence of PON1 and PON3 in brain astrocytes does not seem coincidental and could suggest a role of PON1 and PON3 in astrocyte cholesterol efflux that is highly dysregulated by the AD pathology. In fact, dysregulation of brain cholesterol homeostasis has been associated with neurodegeneration [42], and is considered the third hallmark of AD.

Microglia are brain-resident macrophages that interact with all central nervous system components and have an important role in brain development, homeostasis and disease [43]. Although mainly produced by astrocytes, microglia can also synthesize apolipoprotein E (ApoE), which plays a major role in brain cholesterol transport [44], as well as cholesterol synthesis. They also express ABCA-1 and participate in cholesterol efflux to ApoE-containing HDL-like particles [45]. In patients with AD, higher number of reactive microglia have been detected surrounding and phagocytosing A $\beta$  plaques, compared with healthy subjects [46]. This neuroprotective “microglial barrier” regulates amyloid compaction and reduction of neurotoxic fibrils to surrounding neural structures. Dysregulation of lipid metabolism in AD results in accumulation of cholesterol and decreased A $\beta$  phagocytosis in microglia, leading to accumulation of A $\beta$  plaques [45]. Our findings of PON3 co-localization in microglia of mice with AD pathology may indicate promotion of cholesterol efflux, as speculated in astrocytic PON1 and PON3.

The inflammatory response observed in AD and other neurodegenerative diseases leads to production of reactive oxygen species (ROS) by activated astrocytes and microglia, contributing to the increased levels of oxidative stress reported in neurodegenerative diseases [47,48]. Thus, the suggested localization of PON1 and PON3 in astrocytes, and observed co-localization of PON3 in microglia indicate a potential antioxidant role of PON1 and PON3 in decreasing levels of ROS and/or preventing lipid peroxidation in these cell types in AD pathology.

This is a descriptive study that shows for the first time the presence of PON1 and PON3 in A $\beta$  plaques and in star-shaped cells surrounding these A $\beta$  plaques in mice. These results are preliminary but reinforce the hypothesis that HDLs act as delivery carriers of PON1 and PON3 from the liver to areas of high levels of oxidative stress and inflammation, and suggest that PON1 and PON3 have a yet-to-explore role in astrocytes, microglia and the AD pathology, which opens a new line of research on the potential role played by the PON family members in this and other neurodegenerative diseases.

**Author Contributions:** Conceptualization, J.G.S., J.M., J.C. and M.T.C.; methodology, J.G.S. and J.M.; validation, J.M., I.R., J.C. and M.T.C.; investigation, J.G.S., J.M., I.R., J.C. and M.T.C.; resources, M.M., B.M. and M.T.C.; writing—original draft preparation, J.G.S., J.M., J.C., M.T.C.; writing—review and editing, J.M., I.R., M.M., B.M.,



J.J., J.C. and M.T.C.; supervision, M.M., B.M., J.J., J.C. and M.T.C.; funding acquisition, J.M., J.C. and M.T.C. All authors have read and agreed to the published version of the manuscript.

**Funding:** This research was funded by the Spanish Ministry of Science and Innovation, grant number SEJ2006-15628-C02-02; the Spanish *Instituto de Salud Carlos III*, grant number FIS 05/1607; and the Spanish *Generalitat de Catalunya*, grant number FI 05/00068 (J.M.). During the preparation of the manuscript, J.M. was supported in part by the National Institutes of Health, grant P50 AG05136.

**Acknowledgments:** The authors would like to thank Dr. Carmen Maestre-Martínez for her technical support and Mrs. Monica Monterde for her assistance in brain paraffin processing and tissue sectioning.

**Conflicts of Interest:** The authors declare no conflict of interest. The funders had no role in the design of the study; in the collection, analyses, or interpretation of data; in the writing of the manuscript, or in the decision to publish the results.

## References

1. *Global action plan on the public health response to dementia 2017–2025*; Geneva: World Health Organization, 2017; ISBN 978-92-4-151348-7.
2. Metsaars, W.P.; Hauw, J.-J.; van Welsem, M.E.; Duyckaerts, C. A grading system of Alzheimer disease lesions in neocortical areas. *Neurobiol. Aging* **2003**, *24*, 563–572, doi:10.1016/s0197-4580(02)00134-3.
3. Ridge, P.G.; Ebbert, M.T.W.; Kauwe, J.S.K. Genetics of Alzheimer's disease. *Biomed Res Int* **2013**, *2013*, 254954, doi:10.1155/2013/254954.
4. Rajasekhar, K.; Chakrabarti, M.; Govindaraju, T. Function and toxicity of amyloid beta and recent therapeutic interventions targeting amyloid beta in Alzheimer's disease. *Chem. Commun. (Camb.)* **2015**, *51*, 13434–13450, doi:10.1039/c5cc05264e.
5. Santos, C.Y.; Snyder, P.J.; Wu, W.-C.; Zhang, M.; Echeverria, A.; Alber, J. Pathophysiologic relationship between Alzheimer's disease, cerebrovascular disease, and cardiovascular risk: A review and synthesis. *Alzheimers Dement (Amst)* **2017**, *7*, 69–87, doi:10.1016/j.dadm.2017.01.005.
6. Hsiao, K.; Chapman, P.; Nilsen, S.; Eckman, C.; Harigaya, Y.; Younkin, S.; Yang, F.; Cole, G. Correlative memory deficits, A $\beta$  elevation, and amyloid plaques in transgenic mice. *Science* **1996**, *274*, 99–102, doi:10.1126/science.274.5284.99.
7. Pappolla, M.A.; Chyan, Y.J.; Omar, R.A.; Hsiao, K.; Perry, G.; Smith, M.A.; Bozner, P. Evidence of oxidative stress and in vivo neurotoxicity of beta-amyloid in a transgenic mouse model of Alzheimer's disease: a chronic oxidative paradigm for testing antioxidant therapies in vivo. *Am. J. Pathol.* **1998**, *152*, 871–877.
8. Mackness, M.I. 'A'-esterases. Enzymes looking for a role? *Biochem. Pharmacol.* **1989**, *38*, 385–390, doi:10.1016/0006-2952(89)90376-6.
9. Hassett, C.; Richter, R.J.; Humbert, R.; Chapline, C.; Crabb, J.W.; Omiecinski, C.J.; Furlong, C.E. Characterization of cDNA clones encoding rabbit and human serum paraoxonase: the mature protein retains its signal sequence. *Biochemistry* **1991**, *30*, 10141–10149, doi:10.1021/bi00106a010.
10. Reddy, S.T.; Wadleigh, D.J.; Grijalva, V.; Ng, C.; Hama, S.; Gangopadhyay, A.; Shih, D.M.; Lusis, A.J.; Navab, M.; Fogelman, A.M. Human paraoxonase-3 is an HDL-associated enzyme with biological activity similar to paraoxonase-1 protein but is not regulated by oxidized lipids. *Arterioscler. Thromb. Vasc. Biol.* **2001**, *21*, 542–547, doi:10.1161/01.atv.21.4.542.
11. Rothem, L.; Hartman, C.; Dahan, A.; Lachter, J.; Eliakim, R.; Shamir, R. Paraoxonases are associated with intestinal inflammatory diseases and intracellularly localized to the endoplasmic reticulum. *Free Radic. Biol. Med.* **2007**, *43*, 730–739, doi:10.1016/j.freeradbiomed.2007.05.003.

12. Schweikert, E.-M.; Devarajan, A.; Witte, I.; Wilgenbus, P.; Amort, J.; Förstermann, U.; Shabazian, A.; Grijalva, V.; Shih, D.M.; Farias-Eisner, R.; et al. PON3 is upregulated in cancer tissues and protects against mitochondrial superoxide-mediated cell death. *Cell Death Differ.* **2012**, *19*, 1549–1560, doi:10.1038/cdd.2012.35.
13. Deakin, S.; Leviev, I.; Gomaschi, M.; Calabresi, L.; Franceschini, G.; James, R.W. Enzymatically active paraoxonase-1 is located at the external membrane of producing cells and released by a high affinity, saturable, desorption mechanism. *J. Biol. Chem.* **2002**, *277*, 4301–4308, doi:10.1074/jbc.M107440200.
14. Efrat, M.; Aviram, M. Macrophage paraoxonase 1 (PON1) binding sites. *Biochem. Biophys. Res. Commun.* **2008**, *376*, 105–110, doi:10.1016/j.bbrc.2008.08.106.
15. Deakin, S.P.; Bioletto, S.; Bochaton-Piallat, M.-L.; James, R.W. HDL-associated paraoxonase-1 can redistribute to cell membranes and influence sensitivity to oxidative stress. *Free Radic. Biol. Med.* **2011**, *50*, 102–109, doi:10.1016/j.freeradbiomed.2010.09.002.
16. Mackness, B.; Hunt, R.; Durrington, P.N.; Mackness, M.I. Increased immunolocalization of paraoxonase, clusterin, and apolipoprotein A-I in the human artery wall with the progression of atherosclerosis. *Arterioscler. Thromb. Vasc. Biol.* **1997**, *17*, 1233–1238, doi:10.1161/01.atv.17.7.1233.
17. Rodrigo, L.; Hernández, A.F.; López-Caballero, J.J.; Gil, F.; Pla, A. Immunohistochemical evidence for the expression and induction of paraoxonase in rat liver, kidney, lung and brain tissue. Implications for its physiological role. *Chem. Biol. Interact.* **2001**, *137*, 123–137, doi:10.1016/s0009-2797(01)00225-3.
18. Marsillach, J.; Mackness, B.; Mackness, M.; Riu, F.; Beltrán, R.; Joven, J.; Camps, J. Immunohistochemical analysis of paraoxonases-1, 2, and 3 expression in normal mouse tissues. *Free Radic. Biol. Med.* **2008**, *45*, 146–157, doi:10.1016/j.freeradbiomed.2008.03.023.
19. Marsillach, J.; Camps, J.; Beltran-Debón, R.; Rull, A.; Aragones, G.; Maestre-Martínez, C.; Sabench, F.; Hernández, M.; Castillo, D.D.; Joven, J.; et al. Immunohistochemical analysis of paraoxonases-1 and 3 in human atheromatous plaques. *Eur. J. Clin. Invest.* **2011**, *41*, 308–314, doi:10.1111/j.1365-2362.2010.02411.x.
20. Furlong, C.E.; Richter, R.J.; Li, W.-F.; Brophy, V.H.; Carlson, C.; Rieder, M.; Nickerson, D.; Costa, L.G.; Ranchalis, J.; Lusic, A.J.; et al. The Functional Consequences of Polymorphisms in the Human PON1 Gene. In *The Paraoxonases: Their Role in Disease Development and Xenobiotic Metabolism*; Mackness, B., Mackness, M., Aviram, M., Paragh, G., Eds.; Proteins And Cell Regulation; Springer Netherlands: Dordrecht, 2008; pp. 267–281 ISBN 978-1-4020-6561-3.
21. Furlong, C.E.; Marsillach, J.; Jarvik, G.P.; Costa, L.G. Paraoxonases-1, -2 and -3: What are their functions? *Chem Biol Interact* **2016**, *259*, 51–62, doi:10.1016/j.cbi.2016.05.036.
22. Khersonsky, O.; Tawfik, D.S. Structure-reactivity studies of serum paraoxonase PON1 suggest that its native activity is lactonase. *Biochemistry* **2005**, *44*, 6371–6382, doi:10.1021/bi047440d.
23. Draganov, D.I.; Teiber, J.F.; Speelman, A.; Osawa, Y.; Sunahara, R.; La Du, B.N. Human paraoxonases (PON1, PON2, and PON3) are lactonases with overlapping and distinct substrate specificities. *J. Lipid Res.* **2005**, *46*, 1239–1247, doi:10.1194/jlr.M400511-JLR200.
24. Aviram, M.; Rosenblat, M. Paraoxonases 1, 2, and 3, oxidative stress, and macrophage foam cell formation during atherosclerosis development. *Free Radical Biology and Medicine* **2004**, *37*, 1304–1316, doi:10.1016/j.freeradbiomed.2004.06.030.
25. Ng Carey J.; Bourquard Noam; Hama Susan Y.; Shih Diana; Grijalva Victor R.; Navab Mohamad; Fogelman Alan M.; Reddy Srinivasa T. Adenovirus-Mediated Expression of Human Paraoxonase 3 Protects Against the Progression of Atherosclerosis in Apolipoprotein E-Deficient Mice. *Arteriosclerosis, Thrombosis, and Vascular Biology* **2007**, *27*, 1368–1374, doi:10.1161/ATVBAHA.106.134189.

26. Liu, Y.; Mackness, B.; Mackness, M. Comparison of the ability of paraoxonases 1 and 3 to attenuate the in vitro oxidation of low-density lipoprotein and reduce macrophage oxidative stress. *Free Radical Biology and Medicine* **2008**, *45*, 743–748, doi:10.1016/j.freeradbiomed.2008.05.024.
27. Zhang, C.; Peng, W.; Wang, M.; Zhu, J.; Zang, Y.; Shi, W.; Zhang, J.; Qin, J. Studies on protective effects of human paraoxonases 1 and 3 on atherosclerosis in apolipoprotein E knockout mice. *Gene Therapy* **2010**, *17*, 626–633, doi:10.1038/gt.2010.11.
28. Camps, J.; Marsillach, J.; Joven, J. The paraoxonases: role in human diseases and methodological difficulties in measurement. *Crit Rev Clin Lab Sci* **2009**, *46*, 83–106, doi:10.1080/10408360802610878.
29. Cervellati, C.; Valacchi, G.; Tisato, V.; Zuliani, G.; Marsillach, J. Evaluating the link between Paraoxonase-1 levels and Alzheimer's disease development. *Minerva Med.* **2019**, *110*, 238–250, doi:10.23736/S0026-4806.18.05875-5.
30. Bennett, S.; Grant, M.M.; Aldred, S. Oxidative stress in vascular dementia and Alzheimer's disease: a common pathology. *J. Alzheimers Dis.* **2009**, *17*, 245–257, doi:10.3233/JAD-2009-1041.
31. Cheignon, C.; Tomas, M.; Bonnefont-Rousselot, D.; Faller, P.; Hureau, C.; Collin, F. Oxidative stress and the amyloid beta peptide in Alzheimer's disease. *Redox Biol* **2018**, *14*, 450–464, doi:10.1016/j.redox.2017.10.014.
32. Butterfield, D.A.; Boyd-Kimball, D. Oxidative Stress, Amyloid- $\beta$  Peptide, and Altered Key Molecular Pathways in the Pathogenesis and Progression of Alzheimer's Disease. *J. Alzheimers Dis.* **2018**, *62*, 1345–1367, doi:10.3233/JAD-170543.
33. Kontush, A.; Atwood, C.S. Amyloid-beta: phylogenesis of a chameleon. *Brain Res. Brain Res. Rev.* **2004**, *46*, 118–120, doi:10.1016/j.brainresrev.2004.05.001.
34. Bassett, C.N.; Montine, T.J. Lipoproteins and lipid peroxidation in Alzheimer's disease. *J Nutr Health Aging* **2003**, *7*, 24–29.
35. Markesbery, W.R.; Carney, J.M. Oxidative alterations in Alzheimer's disease. *Brain Pathol.* **1999**, *9*, 133–146, doi:10.1111/j.1750-3639.1999.tb00215.x.
36. Lovell, M.A.; Ehmann, W.D.; Butler, S.M.; Markesbery, W.R. Elevated thiobarbituric acid-reactive substances and antioxidant enzyme activity in the brain in Alzheimer's disease. *Neurology* **1995**, *45*, 1594–1601, doi:10.1212/wnl.45.8.1594.
37. Wills, A.-M.; Landers, J.E.; Zhang, H.; Richter, R.J.; Caraganis, A.J.; Cudkowicz, M.E.; Furlong, C.E.; Brown, R.H. Paraoxonase 1 (PON1) organophosphate hydrolysis is not reduced in ALS. *Neurology* **2008**, *70*, 929–934, doi:10.1212/01.wnl.0000305956.37931.dd.
38. Castellazzi, M.; Trentini, A.; Romani, A.; Valacchi, G.; Bellini, T.; Bonaccorsi, G.; Fainardi, E.; Cavicchio, C.; Passaro, A.; Zuliani, G.; et al. Decreased arylesterase activity of paraoxonase-1 (PON-1) might be a common denominator of neuroinflammatory and neurodegenerative diseases. *Int. J. Biochem. Cell Biol.* **2016**, *81*, 356–363, doi:10.1016/j.biocel.2016.06.008.
39. Romani, A.; Trentini, A.; van der Flier, W.M.; Bellini, T.; Zuliani, G.; Cervellati, C.; Teunissen, C.E. Arylesterase Activity of Paraoxonase-1 in Serum and Cerebrospinal Fluid of Patients with Alzheimer's Disease and Vascular Dementia. *Antioxidants* **2020**, *9*, 456, doi:10.3390/antiox9050456.
40. Balazs, Z.; Panzenboeck, U.; Hammer, A.; Sovic, A.; Quehenberger, O.; Malle, E.; Sattler, W. Uptake and transport of high-density lipoprotein (HDL) and HDL-associated alpha-tocopherol by an in vitro blood-brain barrier model. *J Neurochem* **2004**, *89*, 939–950, doi:10.1111/j.1471-4159.2004.02373.x.
41. Fung, K.Y.; Wang, C.; Nyegaard, S.; Heit, B.; Fairn, G.D.; Lee, W.L. SR-BI Mediated Transcytosis of HDL in Brain Microvascular Endothelial Cells Is Independent of Caveolin, Clathrin, and PDZK1. *Front Physiol* **2017**, *8*, 841, doi:10.3389/fphys.2017.00841.



42. Blain, J.-F.; Poirier, J. Cholesterol homeostasis and the pathophysiology of Alzheimer's disease. *Expert Rev Neurother* **2004**, *4*, 823–829, doi:10.1586/14737175.4.5.823.
43. Li, Q.; Barres, B.A. Microglia and macrophages in brain homeostasis and disease. *Nat Rev Immunol* **2018**, *18*, 225–242, doi:10.1038/nri.2017.125.
44. Mathys, H.; Davila-Velderrain, J.; Peng, Z.; Gao, F.; Mohammadi, S.; Young, J.Z.; Menon, M.; He, L.; Abdurrob, F.; Jiang, X.; et al. Single-cell transcriptomic analysis of Alzheimer's disease. *Nature* **2019**, *570*, 332–337, doi:10.1038/s41586-019-1195-2.
45. Loving, B.A.; Bruce, K.D. Lipid and Lipoprotein Metabolism in Microglia. *Front Physiol* **2020**, *11*, doi:10.3389/fphys.2020.00393.
46. Yuan, P.; Condello, C.; Keene, C.D.; Wang, Y.; Bird, T.D.; Paul, S.M.; Luo, W.; Colonna, M.; Baddeley, D.; Grutzendler, J. TREM2 Haplodeficiency in Mice and Humans Impairs the Microglia Barrier Function Leading to Decreased Amyloid Compaction and Severe Axonal Dystrophy. *Neuron* **2016**, *90*, 724–739, doi:10.1016/j.neuron.2016.05.003.
47. Su, B.; Wang, X.; Nunomura, A.; Moreira, P.I.; Lee, H.; Perry, G.; Smith, M.A.; Zhu, X. Oxidative Stress Signaling in Alzheimer's Disease. *Curr Alzheimer Res* **2008**, *5*, 525–532.
48. Simpson, D.S.A.; Oliver, P.L. ROS Generation in Microglia: Understanding Oxidative Stress and Inflammation in Neurodegenerative Disease. *Antioxidants (Basel)* **2020**, *9*, doi:10.3390/antiox9080743.